Published in final edited form as:
Glob Chang Biol. 2023 September ; 29(17): 4793–4810. doi:10.1111/gcb.16817.

Future climate change effects on U.S. forest composition may offset benefits of reduced atmospheric deposition of N and S

Christopher M. Clark[1,*], **Jennifer Phelan**[2], **Jeremy Ash**[3], **John Buckley**[2], **James Cajka**[2], **Kevin Horn**[4], **R. Quinn Thomas**[5], **Robert D. Sabo**[1]

[1]US Environmental Protection Agency, Office of Research and Development, Center for Public Health and Environmental Assessment, Washington DC.

[2]RTI International, Research Triangle Park, NC.

[3]US Department of Agriculture, US Forest Service, Region 8, Ashville, NC.

[4]Virginia Polytechnical University, Department of Forest Resources and Environmental Conservation, Blacksburg, VA.

[5]Virginia Polytechnical University, Department of Forest Resources and Environmental Conservation, Blacksburg, VA.

Abstract

Climate change and atmospheric deposition of nitrogen (N) and sulfur (S) are important drivers of forest demography. Here we apply previously-derived growth and survival responses for 94 tree species, representing >90% of the contiguous U.S. forest basal area, to project how changes in mean annual temperature, precipitation, and N and S deposition from 20 different future scenarios may affect forest composition to 2100. We find that under the low climate change scenario (RCP 4.5), reductions in aboveground tree biomass from higher temperatures are roughly offset by increases in aboveground tree biomass from reductions in N and S deposition. However, under the higher climate change scenario (RCP 8.5) the decreases from climate change overwhelm increases from reductions in N and S deposition. These broad trends underlie wide variation among species. We found averaged across temperature scenarios the relative abundance of 60 species were projected to decrease more than 5% and 20 species were projected to increase more than 5%; and reductions of N and S deposition led to a decrease for 13 species and an increase for 40 species. This suggests large shifts in the composition of U.S. forests in the future. Negative climate effects were mostly from elevated temperature and were not offset by scenarios with wetter conditions. We found that by 2100 an estimated 1 billion trees under the RCP 4.5 scenario and 20 billion trees under the RCP 8.5 scenario may be pushed outside the temperature record upon which these relationships were derived. These results may not fully capture future changes in forest composition as several other factors were not included. Overall efforts to reduce atmospheric deposition of N and S will likely be insufficient to overcome climate change impacts on forest demography across much of the United States unless we adhere to the low climate change scenario.

[*]Corresponding author: clark.christopher@epa.gov.

Keywords

climate change; atmospheric deposition; forests; biodiversity; species; demographics

Introduction:

Climate change and atmospheric deposition of nitrogen (N) and sulfur (S) are central drivers of forest tree growth and survival (Horn et al., 2018; Nate G McDowell et al., 2020; Linda H. Pardo et al., 2011; Stanke, Finley, Domke, Weed, & MacFarlane, 2021; Van Houtven et al., 2019; Vose, 2018). There are many emerging signals of climate change in the U.S., including increases in average temperatures, increases in heat waves and heavy precipitation, and increasing drought and wildfires (EPA, 2023). Precipitation shifts are more variable than temperature trends, with increases in precipitation for the east, Midwest, and Pacific Northwest, and decreases in the Southwest (EPA, 2023). Atmospheric deposition of N and S in the U.S., after years of increases beginning in the late 19th and early 20^{th} (Galloway et al., 2004; Lamarque et al., 2010), has been steadily decreasing from successful air quality policies that focus primarily on oxidized sources of N and S (EPA, 2020; Lloret & Valiela, 2016; Zhang et al., 2019). However, N deposition is not decreasing in much of the western U.S., and deposition of reduced N is increasing over some portions of the Midwestern U.S. from increased fertilizer application (Li et al., 2016; Sabo et al., 2019; Zhang et al., 2019). Thus, even today rates of N and S deposition remain well above estimated pre-industrial levels under which these ecosystems evolved (Holland, Dentener, Braswell, & Sulzman, 1999).

Climate change affects tree dynamics through a variety of mechanisms (Nate G McDowell et al., 2020; Vose, 2018). Elevated temperature may increase growth through temperature dependent effects on decomposition and changes in nutrient availability (Melillo et al., 2011), or decrease growth and increase mortality though effects on vapor pressure deficit and hydraulic conductivity if precipitation cannot offset heightened temperatures (Grossiord et al., 2020; Nathan G McDowell & Allen, 2015; Park et al., 2013). Elevated CO_2 is expected to increase growth (R. J. Norby et al., 2005), but this may be contingent on other factors such as nutrient or water availability (Cabon et al., 2022; Luo et al., 2004; Richard J Norby et al., 2002; Walker et al., 2019), or mycorrhizal association (Terrer, Vicca, Hungate, Phillips, & Prentice, 2016). Climate change is also associated with increased frequency and severity of disturbances such as from wildfire and pests which dramatically affect forest survival (K. T. Davis et al., 2019; Hicke, Meddens, & Kolden, 2016; Nate G McDowell et al., 2020; Stanke et al., 2021).

Atmospheric deposition of N and S also impact forests through a variety of mechanisms (Carter et al., 2017; EPA, 2020; M. E. Fenn et al., 2003). S deposition primarily has a negative effect through the process of soil acidification, whereby important base cations (e.g., Ca^{2+}, Mg^{2+}) may be leached from the soil and into surface waters, reducing the ability of the soil to buffer against future acid inputs (EPA, 2020). This can lead to imbalances in foliar chemistry (Boxman et al., 1998; Schaberg et al., 2002) affecting stress responses in trees (Schaberg et al., 2002) and in extreme cases, Al^{3+} release to the soil which is

phytotoxic to root tissue (Cronan et al., 1989), all of which may lead to reductions in growth or survival (Cronan et al., 1989; Mark E Fenn et al., 2020; Horn et al., 2018). N deposition can have both positive and negative effects on forested ecosystems (Aber et al., 1998; Carter et al., 2017; Horn et al., 2018). Because N is commonly limiting in most terrestrial ecosystems (LeBauer & Treseder, 2008), the addition of low levels of N may have a fertilization effect, increasing available N in the soil and subsequently the growth and survival of individual tree species (Aber et al., 1998; Canham & Murphy, 2016; Dietze & Moorcroft, 2011; Horn et al., 2018). However, higher rates of N deposition or chronic N inputs for longer periods of time may lead to N in excess of ecosystem needs (Aber et al., 1998), which can lead to the same acidification effects as S, including cation imbalances and negative effects on growth and survival (Horn et al., 2018; Magill et al., 2004). N deposition may also aggravate effects from secondary stressors, including pest pressures (Bobbink et al., 2010), reduced cold tolerance (Schaberg et al., 2002), and hydraulic cavitation under periods of drought (Fan et al., 2022; Gessler, Schaub, & McDowell, 2017).

Because of the many effects from climate change and N and S deposition on forest tree growth and survival, and because both sets of drivers have deviated from pre-industrial conditions for decades (Galloway et al., 2004; Lamarque et al., 2010; USGCRP, 2017), there are likely changes already underway in the composition of U.S. forests (Van Houtven et al., 2019). These slower changes from shifts in primary drivers are difficult to discern compared with conspicuous changes from extreme events like wildfire and pest outbreaks (Hicke et al., 2016; Stanke et al., 2021). However, changes in temperature, precipitation, and atmospheric deposition impact individual tree species differently, and how synergistic or antagonistic effects across the multiple climate and deposition drivers ultimately aggregate to the forest community now and into the future remains uncertain (Vose, 2018).

Recent research suggests a wide variation in responses at the species level for these drivers. Experimental research on juvenile trees in the northern U.S. found the growth of two species increased with even modest increases in temperature (*Acer rubrum, Acer saccarum*) while the growth of three decreased (*Abies balsamea, Picea glauca and Pinus strobus*) (Reich et al., 2022). Wide variation among tree species responses to atmospheric N deposition has been reported as well, in both the U.S. (Canham & Murphy, 2016; Horn et al., 2018) and EU (Solberg et al., 2009). Even though the direction of effect is typically negative for S deposition because of acidification, there is still wide variation reported among species in their sensitivity (Mark E Fenn et al., 2020; Horn et al., 2018). These divergent response patterns among species lead to changes in composition. A recent observational analysis of eight dominant western species found divergent population trends among species due to differential effects among species from different drivers, leading to increases in *Pseudotsuga menziesii* and *Pinus ponderosa* and decreases in *Abies lasiocarpa*, *Populus tremuloides*, *Picea engelmannii*, and *Pinus contorta* (Stanke et al., 2021). These species-specific differences have uncertain effects on the composition of forests in the future as well and the various ecosystem services that they provide.

In this study, we use species-specific empirical relationships for 94 different tree species to simulate changes in forest composition from 2010 to 2100. We extend a recent assessment that derived relationships between the growth and survival rates of these individual tree

species to various environmental factors (Horn et al., 2018) and use these empirical relationships to drive a simple forest composition model (Van Houtven et al., 2019) to examine the implications of various climate change and air quality scenarios on future forest composition across the contiguous U.S. Five climate change and four atmospheric N and S deposition scenarios were used to calculate the annual growth and survival rates of individual trees across the CONUS from 2010 to 2100. We use these to estimate how forest composition of the current cohort of sampled trees - representing roughly 100 billion U.S. trees - is projected to change at the species and community level under future air quality and climate change scenarios.

Materials and Methods:

Overview of Tree Species Response Curves

Forest Inventory data.—Tree growth, tree survival, and plot-level basal area data were compiled from the Forest Inventory and Analysis (FIA) program database representing the forest cohort from 2000–2016 (accessed on January 24, 2017, FIA phase 2 manual version 6.1; http://www.fia.fs.fed.us/). Tree biomass was estimated from tree DBH measurements multiplied by allometric relationships in (Jenkins, Chojnacky, Heath, & Birdsey, 2003) to estimate aboveground biomass. Aboveground biomass is then multiplied by 0.5 to estimate aboveground C. Tree growth rates were calculated from the difference in aboveground C between the latest and first measurement and divided by the elapsed time between measurements to the day. Tree species that had at least 2,000 individual trees after the data filters were applied were retained for both growth and survival analyses. The 1.4 million trees from 94 species modeled in (Horn et al., 2018) represent nearly 100 billion trees in the U.S., representing >90% of trees in most forested areas in the U.S. (Fig. S1). Nonetheless, there were some areas with lower representation from these 94 species, including in the Pacific Northwest (75–90%), California, and the Southwest (<50%) (Fig. S1). Thus, some important tree species are omitted and require additional study (e.g., Sequoia sempervirens [redwood, <1500 samples]). The probability of tree survival was calculated from the first live measurement to the last live measurement or to the first measurement recorded as dead for each tree inventoried. Trees that were recorded as dead at both measurement inventories and trees that were harvested were excluded from the survival analysis.

Predictor data: Climate, deposition, size, and competition.—There were six predictors that were related to the rate of growth or survival for each individual tree: mean annual temperature (T), mean annual precipitation (P), mean annual total nitrogen deposition (N), mean annual total S deposition (S), tree size (m), and plot-level competition.

To obtain total N and S deposition rates for each tree, we used spatially modeled N and S deposition data from the National Atmospheric Deposition Program's Total Deposition (TDEP) Science Committee (Schwede & Lear, 2014). Annual N and S deposition rates were then averaged from the first year of measurement to the last year of measurement for every tree so that each tree had an individualized average N deposition based on the remeasurement years, and each species had an individualized range of average N deposition exposure based on its distribution. At the time of the analysis, deposition from only 2000–

2014 was available, so we used the 2014 deposition values for the years 2015 and 2016. Monthly mean temperature and precipitation values were obtained in a gridded (4 × 4 km) format from the PRISM Climate Group at Oregon State (Daly et al., 2008) for the CONUS and averaged between measurement periods for each tree in a similar manner. Tree size was represented by aboveground tree C (m, previously described). Because the climate and deposition predictors were tailored to each plot, the years assessed varied by plot, but spanned 2000–2016. Tree competition was represented by a combination two factors: (1) plot basal area (BA) and the basal area of trees larger than the focal tree being modeled (BAL). How all six variables were statistically modeled is discussed below. Many other factors also influence growth and survival of tree species such as ozone, pests, CO_2 concentrations, and forest management. However, these factors were not included in the original growth and survival derivations and so were also not included in their application here. We discuss the implications of this and other factors below.

Modeling tree growth and survival.—We assessed in Horn et al. (2018) multiple models to predict tree growth and survival. Our growth model assumes that there is a potential growth rate (a) that is modified by up to six predictors in our study: temperature, precipitation, N deposition, S deposition, tree size, and competition. The potential full growth model included all six terms (eq. 4 for the general form and eq. 5 for the specific form).

$$G = potentialgrowthrate \times competition \times temperature \times precipitation \times S_{dep} \times N_{dep} \quad \text{(eq. 4)}$$

$$G = a * m^{z} * e^{(c_1 * BAL + c_2 * \ln(BA))} * e^{-0.5 * \left(\frac{\ln(T/t_1)}{t_2}\right)^2} * e^{-0.5 * \left(\frac{\ln(P/p_1)}{p_2}\right)^2} * e^{-0.5 * \left(\frac{\ln(N/n_1)}{n_2}\right)^2} * e^{-0.5 * \left(\frac{\ln(S/s_1)}{s_2}\right)^2} \quad \text{(eq. 5)}$$

To predict growth, we considered each tree species to have an optimal growth rate that was a power function of its size (m), where size is in units of aboveground carbon (kg C/tree), a is a fitted parameter, and z is a fitted parameter. Competition between trees was modeled as a function of plot basal area (BA) and the basal area of trees larger than that of the tree of interest (BAL) similar to the methods of (Pukkala, Lähde, & Laiho, 2009), where c_1 and c_2 were fitted parameters, and BA and BAL were observed based on plot conditions. The environmental factors (temperature [T], precipitation [P], S deposition [S], and N deposition [N]) were interpolated per the above procedures at the plot location. The effect of the environmental factors on growth were modeled as two-term lognormal functions (e.g., t_1 and t_2 are fitted parameters for the effect of temperature on growth, p_1 and p_2 are two term parameters for the effect of precipitation on growth, etc.). The two-term lognormal functions allowed for flexibility in both the location of the peak (controlled by the value of t_1, p_1, n_1, and s_1), and the steepness of the curve (controlled by t_2, p_2, n_2, and s_2). Thus, in the parlance of critical loads (L.H. Pardo et al., 2011) the estimates of n_1 and s_1 are reasonable

estimates of the critical loads for N and S, respectively. The full growth model with all terms potentially present is shown in equation 5.

We examined a total of six different growth models: (1) a full model with all six terms (eq. 5), (2) the full model but without the N deposition term, (3) the full model but without the S deposition term, (4) the full model but without both N or S deposition terms, and (5) a null model that estimated a single parameter for the mean growth parameter (*a*).

The annual probability of survival (P(s)) was estimated similarly as growth, except that the probability was a function of time and we explored two different representations for competition. The general form of the model is shown in equation 6, and the full survival model in equations 7 and 8 for the two competition forms.

$$P(s) = [a \cdot \text{size} \times competition \times temperature \times precipitation \times N_{dep} \times S_{dep}]^{time} \quad \text{(eq. 6)}$$

$$P(s) = \left[a * \left[\left(\left(1 - zc_1 e^{-zc_2 * m}\right) * e^{-zc_3 * m^{zc_4}}\right)\left(e^{-br_1 * BA_{ratio}{}^{br2} * BA^{br_3}}\right)\right] * e^{-0.5 * \left(\frac{ln\left(T/t_1\right)}{t_2}\right)^2} * e^{-0.5 * \left(\frac{ln\left(P/p_1\right)}{p_2}\right)^2} * e^{-0.5 * \left(\frac{ln\left(N/n_1\right)}{n_2}\right)^2} * e^{-0.5 * \left(\frac{ln\left(S/s_1\right)}{s_2}\right)^2}\right]^{time} \quad \text{(eq. 7)}$$

$$P(s) = \left[a * \left(e^{-0.5 * \left(\frac{ln\left(m/m_1\right)}{m_2}\right)^2} * -0.5 * \left(\frac{ln\left(BA/ba_1\right)}{ba_2}\right)^2 * -0.5 * \left(\frac{ln\left(BAL + 1/bl_1 + 1\right)}{bl_2}\right)^2\right) * e^{-0.5 * \left(\frac{ln\left(T/t_1\right)}{t_2}\right)^2} * e^{-0.5 * \left(\frac{ln\left(P/p_1\right)}{p_2}\right)^2} * e^{-0.5 * \left(\frac{ln\left(N/n_1\right)}{n_2}\right)^2} * e^{-0.5 * \left(\frac{ln\left(S/s_1\right)}{s_2}\right)^2}\right]^{time} \quad \text{(eq. 8)}$$

A total of nine survival models were examined: four using the formulation for size and competition in eq. 7 (with the same combinations of predictors as above for growth), four using formulation for size and competition in eq. 8, and a null survival model in which a mean annual estimate of survival (*a*) was raised to the exponent of the elapsed time.

Parameters for each of the growth and survival models above were fit for a given species using maximum likelihood estimates through simulated annealing with 100,000 iterations via the likelihood package (v2.1.1) in Program R. Akaike's Information Criteria (AIC) was estimated for all models. We used the nest overall model as assessed by AIC. Horn et al. (2018) focused on the "best and most parsimonious model" which meant the model with the least parameters among the set of comparable models (i.e., those within a delta AIC of 2.0 of the best model, (Burnham, 2002)). Additional review of all the models in Horn et al. (2018) for this project revealed that for a small number of species, the most parsimonious models resulted in N-only models beating out models with both N and S, and S-only models beating out models with both N and S. Because N and S are often correlated, the N term in the N-only model could absorb some of the statistical information in S deposition and thus the

N relationship could shift from positive or unimodal to flat or negative. Opposite shifts could occur for S (i.e., it could become flat or less negative when N was omitted). The degree of shift was related to the degree of correlation between N and S for that species. Because we hypothesize both N and S deposition matter, we decided to use the best overall model as determined by AIC which often was the model with both terms. The variation explained in the models in Horn et al. (2018) was good for growth (R^2 averaged 24% for the 94 species +/− 15% standard deviation) and was not reported for survival. Additional details can be found in Horn et al. (2018).

This work is part of a large multi-year effort by the U.S. Environmental Protection Agency to better understand how forest communities may be impacted by changes in climate and atmospheric deposition (C. M. T. Clark, R Quinn; Horn, Kevin J, 2023; LeDuc et al., 2022; Phelan et al., 2016; Van Houtven et al., 2019). Similar to other studies (Van Houtven et al., 2019), a single cohort of trees was modeled, and only mean annual temperature and mean annual precipitation were included as climate predictors in our assessments (limitations of this discussed below).

Application of Response Curves to Estimate Changes in Forest Composition

Initial tree database—We assembled an initial cohort of live trees for the project. The original database from Horn et al. (2018) upon which the response curves were derived required *remeasured* trees for estimates of growth and survival (i.e., two or more time points). *Application* of those response curves onto existing trees does not require trees to have been remeasured, thus the dataset used here is an expansion of that in (Horn et al., 2018) including areas with trees that had only been measured once. This database consists of tree- and plot- specific data from the U.S. Forest Service Forest Inventory and Analysis (FIA) program assembled for the survival models in Horn et al. (2018) but augmented to include all live trees from the most recent measurement between 2000–2016. It includes tree and plot data for 124,431 plots, 352 species, and 2,851,772 individual trees across the conterminous U.S. As per the FIA definition of “tree” and for consistency with Horn et al. (2018), only stems ≥12.7 cm at 1.3 m height are included in the tree database; saplings and trees smaller than 12.7 cm in diameter were not included. Measured trees in the FIA represent a larger population of trees across the landscape through “expansion factors.” With the expansion factors, the trees in our initial tree database represent roughly 100 billion trees across the U.S. Tree numbers were expanded to the county-level, using FIA tree- and plot-specific expansion factors and equations (O’Connell et al., 2017). Although the tree data are for conditions measured in 2000–2016, all trees are assumed to be their reported FIA biomass in the model start year of 2010 for consistency with the future deposition and climate scenarios.

Future Deposition and Climate Scenarios—Total Deposition estimates (TDEP) for 2009–2011 served as the source of the current N and S deposition estimates (Schwede & Lear, 2014). Future deposition scenarios were from CMAQ v5.0.2 (Zhang et al., 2019) total N and S deposition estimates applied as scaling factors (determined for each plot) to TDEP to estimate reductions in deposition associated with the policy-based reductions in emissions.

Constant deposition scenario (D_0, Fig. 1) – this scenario represented the plot-specific 3-year average (2009–2011) N and S deposition levels held constant from 2010–2100.

N deposition reduction scenario (D_N, Fig. 1) – This scenario represented policy-based anticipated reductions in N deposition while maintaining S deposition at 2009–2011 levels. Reductions in total N deposition were based on the differences between two years (2011 and 2028) from the CMAQ model developed in Zhang et al. (2019) for total N deposition converted into plot-specific % change in deposition. These represented the best available estimates for anticipated changes in N deposition for the U.S. to support policymaking at the time (EPA, 2013a, 2013b). These % changes in deposition were then applied to the plot-specific TDEP N deposition (D_0), as linear declines in annual TDEP N deposition from 2011 to 2028. Total N deposition in 2028 served as the estimate of annual N deposition from 2029 to 2100. Total S deposition remained at the 2009–2011 level for the full simulation (2010–2100).

S deposition reduction scenario (D_S, Fig. 1) – Similar to D_N, this scenario represented policy-based reductions in S deposition from 2010–2028 while maintaining N deposition at 2009–2011 levels. S deposition after 2028 was held constant.

N and S deposition reduction scenario (D_{NS}, Fig. 1) – This scenario represented policy-based reductions in both N and S deposition per the above procedures from D_N and D_S.

The five climate scenarios included current climate and four future climate scenarios. Each of these provided estimates of mean annual precipitation and average annual temperature that were then used in the growth and survival equations above (eq. 4–8) for the forest model. Climate normals from PRISM (http://www.prism.oregonstate.edu/) served as the source of current temperature and precipitation estimates for each plot. The four future climate scenarios were based on four different Earth System Models (ESMs) from two IPCC AR5 Representative Concentration Pathway (RCP) emission scenarios (Fig. 1). At the time of the analysis IPCC AR6 estimates were not yet available. The IPCC AR5 estimates have been statistically downscaled as Localized Constructed Analogs (LOCA) datasets (Pierce, Cayan, & Thrasher, 2014) to represent changes of potential temperatures and precipitation at locations across the CONUS. Changes in climate associated with each of these future scenarios were applied as scaling factors (determined for each plot) to the PRISM data to estimate changes in annual temperature and precipitation predicted by the future scenarios.

Constant climate scenario (CC, Fig. 1) – this scenario represented recent climate maintained over time and consisted of plot-specific 30-year average (1981–2010) 4-km PRISM temperature and precipitation estimates repeated from 2010–2100.

Modest climate change ($C_{4.5}$, Fig. 1) – This scenario represented potential future climate from RCP 4.5, using a central estimate from the collection of models available (Fig. 1). At each plot location, the differences between 10-year averages for 2006–2015 and 2090–2099 of the modeled precipitation and temperature

were extracted. These estimates were used to calculate the percent change in precipitation and degree change of temperature projected for at each plot. These changes (percent for precipitation and degrees for temperature) were then be applied to the plot-specific PRISM "constant" climate conditions, as linear changes in temperature and precipitation from 2010 to 2100.

Moderate climate change, wet ($C_{8.5, mod}$, Fig. 1) – This scenario represented potential future climate from RCP 8.5, using an estimate from the cooler end of the temperature range and moderate precipitation for RCP 8.5 (Fig. 1). A linear change for temperature and precipitation from 2010 to 2100 was then estimated for each plot using the same methods as described above for $C_{4.5}$.

Severe climate change, wet ($C_{8.5, wet}$, Fig. 1) – This scenario represented potential future climate from RCP 8.5, using an estimate from the wetter end of the precipitation range (Fig. 1). A linear change for temperature and precipitation from 2010 to 2100 was then estimated for each plot using the same methods as described above for $C_{4.5}$.

Severe climate change, dry ($C_{8.5, dry}$, Fig. 1) – This scenario represented potential future climate from RCP 8.5, using an estimate from the drier end of the precipitation range (Fig. 1). A linear change for temperature and precipitation from 2010 to 2100 was then estimated for each plot using the same methods as described above for $C_{4.5}$.

Total annual N and S deposition, annual precipitation, and average annual temperature for the deposition and climate scenarios were converted into 10-year averages (2010–2019….2080–2089). These 10-year deposition, precipitation, and temperature averages served as the 20 deposition – climate scenario input data for the Forest Composition Model (described further below).

Forest Model—The species-specific growth and survival equations published in Horn et al. (2018) were applied to the trees in the initial tree database. We used the same modeling approach as in van Houtven et al. (2019), but with more species and for the CONUS. Only tree species with ≥2000 records (i.e., individual tree data) for the growth and survival models were examined, and only the response curves from the best statistical models (i.e., those with delta AIC values of 0) were used. Therefore, only 94 of the 352 species included in the initial tree database were modeled, totaling 2.6 million trees. The 94 modeled species were found on 120,159 of the 124,731 FIA plots (i.e., 96.3%) in the initial tree database, and on average, represented 93.2% of plot basal area (Fig. S1).

The initial tree database served as the source of the starting tree size and sub-plot basal area model input data, and the deposition and climate scenarios (previously described) were the sources of the precipitation, temperature, and N and S deposition estimates. All model input data were at the plot- or tree-level. Starting tree size was the aboveground biomass (kg C) of the tree at the beginning of the 10-year time step. Sub-plot basal area was calculated as the sum of the basal area of all modeled trees (that increase in size and diameter with each time step) and non-modeled trees. Non-modeled tree biomass (i.e., those of species other than the 94 modeled species) were held constant at the 2010 biomass values). This approach was also

applied to the calculations of sub-plot basal area of all trees larger than the tree of interest, as needed.

The forest composition model estimated changes in above-ground biomass (i.e., growth) and survival in 10-year time steps from 2010–2100 using the best models from Horn et al. (2018) for each of the 20 scenarios (Fig. 1). For each time step, individual tree growth and survival (for the 94 species) were modeled at the sub-plot level, with individual tree biomass and proportion of surviving individuals at the end of the previous time step serving as the starting conditions for the next time step. Growth was modeled as an annual rate (using starting tree size and basal area estimates and 10-year average deposition and climate estimates) multiplied by 10. Survival was modeled as a 10-year probability. Only modeled trees grew and died. The remaining 258 non-modeled tree species are much rarer across the landscape and remained the same size for the full simulation. In addition, to prevent forecasting growth and survival beyond the empirical records used to establish the models, the growth and survival estimates were restricted to the observed ranges from Horn et al. (2018). The empirical data ranges were from the growth equations because they are the most conservative. Once conditions (tree size, N deposition, S deposition, precipitation, temperature, sub-plot basal area and sub-plot basal area of all trees larger than the tree of interest) were outside the training data ranges, annual growth and survival were held constant at the species-specific upper or lower limit for that parameter and that tree was flagged. Thus, we did not extrapolate the response curves beyond the data from which they were derived. Likewise, to prevent individual trees from growing beyond observed sizes, all trees were modeled to stop growing (i.e., individual tree growth of a species was set to 0 kg/yr) once they reached the largest recorded biomass for that species within the USFS FIA database. However, only 0.05–0.11% of the trees (expanded to county level) reached their species-specific maximum biomass and ceased growth during the 2010–2100 period. Many trees, however, reached the edges of the training data for temperature and deposition (discussed below). Sub-plots exceeding recorded basal areas was also a concern, but in 2100 none of the plots had a basal area greater than the largest sub-plot basal area recorded in the FIA database. Lastly, predicted survival rates resulted in some trees being reduced to less than 1 individual at the county level. Similarly, very low trees per hectare counts (approximate 0.00025 trees per ha) for an individual tree resulted in some survival equation predictions returning an “error”. In these situations, the tree was recorded as dead, thereby representing 0 tph at the county level in the next model time step.

Estimating changes in forest composition—Abundances by species were expanded to the county using standard FIA expansion factors (USFS, 2018) and then summed to the CONUS. Differences in composition between scenarios were assessed at the national level by species using differences in relative abundances in the final decade of the simulation (i.e., 2090–2100). Differences in composition were also assessed at the county level by species and for the forest community as a whole using a percent difference metric. The compositional difference (CD) for one county at end-of-century between two scenarios was estimated as the pairwise sum of minimum percent abundances by species (equation 9).

$$CD_{j,k,l}(\%) = 100 - \sum_{i}^{N} \min(Ps_{i,j,k}, Ps_{i,j,l})$$

(eq. 9)

Where $CD_{j,k,l}$ is the compositional difference in county j between scenarios k and l, N is the number of species in county j, and $Ps_{i,j,k}$ and $Ps_{i,j,l}$, are the relative abundances (in percent) of species i and county j, comparing between scenarios k and l. For example, if a county had three species under one scenario (e.g., Ps_1=50%, Ps_2=25%, Ps_3=25%) and three under another scenario that only partly overlapped (e.g., Ps_1=80%, Ps_2=10%, Ps_4=10%), the compositional similarity would be 60% (50% from Ps_1, 10% from Ps_2, and none from Ps_3 or Ps_4 which aren't shared), and the compositional difference would be 40%.

Results:

Across all 20 scenarios we found that the total cohort biomass generally doubled from roughly 30,000 Tg in 2010 to roughly 54,000 – 64,000 Tg across the 20 scenarios in 2100 (Fig. 2, Table S1). There was more biomass accumulation with reductions in S deposition, less biomass accumulation with reductions in N deposition, and more biomass accumulation with the reduction of both N and S (Fig. 2). Greater changes in climate were associated with less biomass accumulation. This appeared to be mostly a temperature effect, as there was little difference between $C_{8.5,\ wet}$ and $C_{8.5,\ dry}$ (both with increases in temperature by roughly 5 $^{\circ}$C, Fig. 1), but both were higher than $C_{8.5\ intermed}$ (+3.5 $^{\circ}$C), which was itself higher than $C_{4.5}$ (+2 $^{\circ}$C). The biomass of all species in 2100 for all 20 scenarios are in Table S1.

For the remainder of the paper, we focus on a subset of scenarios to focus on our research questions of interest on forest composition. We omit further discussion of $C_{8.5,\ intermed}$, since it is intermediate to $C_{4.5}$, and the other two $C_{8.5}$ scenarios (Fig. 1, but see Table S1 for all results). As a reference scenario, we do not use the constant climate and deposition scenario because that is an unlikely future. For the deposition results we use the constant climate scenario as the reference to isolate the deposition effects under the current climate. Changes in deposition are expected to occur over the next few decades (Fig. 1); thus, we use the current climate held climate as the reference to isolate depositional effects. Changes in climate are projected to occur until at least the end of century (USGCRP, 2017). Thus, because lower deposition is the most likely future state for deposition given current policies (Campbell et al., 2019; Zhang et al., 2019), we use the N and S reduction scenario as the baseline for assessing climate effects. Raw results for all scenarios and species are available in the Supplemental Information and Table S1.

At the species level, there was a wide range of projected shifts in relative abundance by 2100 in response to reductions in N and S deposition (Fig. 3, Table S2). By the year 2100 and holding climate constant, reductions in N and S deposition led to a decrease in relative abundance for 27 species and an increase in relative abundance for 67 species (Fig. 3a). Relative abundances of many species varied little in 2100 (41 out of 94 species

projected to change by less than +/−5% with reduction of N and S), while relative abundances of slightly more species (53) varied more substantially with reduction in N and S deposition. The projected relative abundance of thirteen species were lower by 5% or more comparing scenarios D_{NS} with D_0 (Fig. 3a). Of these, 8 species decreased by 5–10% (*Quercus velutina, Lithocarpus densiflorus, Tsuga heterophylla, Acer saccharinum, Carya texana, Taxodium ascendens, Abies amabilis, Pinus palustris*), 4 species decreased by 10–25% (*Prunus serotina, Tsuga mertensiana, Abies grandis, Liriodendron tulipifera*), and 1 species decreased by more than 25% (*Juglans nigra*). Species with lower relative abundances under the D_{NS} scenario appeared to be mostly due to negative effects from lower N deposition (less fertilization, Fig. 3b) offsetting positive or small effects from S deposition reduction (less acidification, Fig. 3c). Of the 40 species that had an increased relative abundance by 5% or more comparing D_{NS} with D_0 in 2100, 12 species increased by 5–10% (Table S2), 19 that increased by 10–25% (Table S2), and 9 that increased by more than 25% (*Ulmus americana, Betula papyrifera, Ulmus rubra, Populus grandidentata, Fraxinus pennsylvanica, Ulmus alata, Acer negundo, Robinia pseudoacacia, Pinus echinata*). Species with higher relative abundances under the D_{NS} scenario appeared to be mostly due to positive effects from lower S deposition (Fig. 3c) which either offset negative effects from lower N deposition or added to positive effects from lower N deposition. For this analysis we focus on changes relative to a reference because a 5% change could be large for a rare species but small for an abundant species (but see Table S1 for biomass to make different comparisons).

For responses to climate change (i.e., MAT and MAP) and assuming reduced N and S deposition (D_{NS}), there were fewer differences among scenarios, with the direction of effect generally consistent for a given species (Fig. 4). Changes under the RCP 4.5 scenario were smaller than the RCP 8.5 scenarios, and changes under the generally hot and dry scenario ($C_{8.5,dry}$) tended to be slightly more negative than hot and wet ($C_{8.5,wet}$). Both observations suggest a strong effect from temperature on tree demographics as reported elsewhere in more mechanistic studies (Nate G McDowell et al., 2020; Park et al., 2013; Reich et al., 2022). That said, the differences in 2100 between hot and wet and hot and dry under RCP 8.5 were <5% for most species (66 spp., Table S2), suggesting a dominant effect from MAT. There were some notable exceptions. For example, *Picea engelmannii, Ulmus rubra,* and *Populus balsamifera* all increased under hot and wet conditions (15.6%, 12.7%, and 17.3% respectively), but decreased under hot and dry conditions (−1.1%, −5.6%, and −7.9% respectively). Most other species showed the same direction of effect between hot and wet versus hot and dry.

Averaging over the three focal climate change scenarios in 2100 ($C_{4.5}$, $C_{8.5,wet}$, $C_{8.5,dry}$) and assuming reductions in N and S deposition (D_{NS}), 69 species had a lower relative abundance in 2100 compared with the no climate change scenario, and 25 had a higher relative abundance. Of the 80 species whose relative abundance differed in either direction by more than 5%, there were 9 species for which relative abundance in 2100 was lower with climate change by 5–10%, 20 species with lower relative abundance by 10–25%, and 31 species with lower relative abundance by more than >25% (Table S2). For species with higher relative abundance under climate change, there were 8, 9, and 3 species that

had a higher relative abundance by 5–10%, 10–25%, and >25%, respectively (Table S2), comparing current climate in 2100 with the average of the climate scenarios in 2100.

Comparing the average response among climate scenarios with the N and S reduction scenario revealed that different species were influenced by different drivers. However, climate change dominated, where 71 species were influenced more by climate change compared with 23 species influenced more by atmospheric deposition (Table S2).

When viewed at a community-level across the CONUS and assuming a constant climate, we found that most of the effects from N or S deposition that may have been significant on a species level (e.g., differences of >5% in 2100 among scenarios, Fig. 3), were obscured when viewed at the community-level across the CONUS (Fig. 5a-c). Across deposition reduction scenarios, almost all counties differed by <5%, with some differing by 5–10%, and only a handful of counties with larger differences. This implies that the changes projected at the species level may be difficult to detect spatially at large scales, but nonetheless add up to significant impacts across the CONUS.

Larger compositional changes were expected from future changes in MAT and MAP. Under the RCP 4.5 scenario, compositional changes compared to a constant climate were relatively small (<5% in most counties, Fig. 5d). However, under the RCP 8.5 scenarios, compositional changes were >10% in many counties, regardless of whether the scenario was hot and wet ($C_{8.5,wet}$, Fig. 5e) or hot and dry ($C_{8.5,dry}$, Fig. 5f). By and large, whether viewed at the individual species or forest composition level, temperature appeared to have the largest effect (differences between 5e and 5f were small by comparison with differences between either of these with 5d). The most likely future is reductions in N and S deposition combined with a yet-uncertain climate future. To explore this, we averaged the climate futures combined with the D_{NS} scenario, which suggested changes in forest composition by 5–10% across most of the U.S. (Fig. S2). County-level results for all species and scenarios discussed are in the SI (Fig. S3 and S4). For example, Fig. S3 shows that *Acer rubrum* (red maple) is projected to decrease in the south and north and increase in the Mid-Atlantic from reduction of N and S deposition, and is projected to decrease in the south and increase in the north from climate change.

Discussion:

The results presented here suggest significant changes in forest biomass and community composition may be underway for U.S. forests. The total aboveground biomass of forests across the CONUS is projected to increase as found for total biomass in other studies (Wear & Coulston, 2015), more so with reductions in N and S deposition and less so with greater changes in MAT. Our study is not a full accounting of C stocks and flows in U.S. forests, but rather is intended to examine changes in composition at the species level. N and S deposition continue to decline in many areas, which we project will benefit many – but not all – tree species. These benefits may be from reduced acidification pressures (from S and also from N) outweighing reduced fertilization effects (from N). This is inferred from comparing the panels of Fig. 3. For species with positive effects from N and S reduction (Fig. 3a, bottom black bars), we can see that although effect of reductions in N deposition (Fig. 3b) could

be positive or negative, the effects of reductions in S deposition (Fig. 3c) were strongly positive and overwhelmed or added to the N effects. Indeed, across all 94 species, assuming a constant climate the effect from D_{NS} was highly correlated with the effect from D_S ($r = 0.638$, $P < 0.0001$), but was uncorrelated with that of D_N ($r = 0.166$, $P = 0.11$).

Effects from reductions in S and N deposition

Reductions in S deposition is a success for U.S. air quality policies after the passage of the Clean Air Act in 1970 and Amendments in 1990 (Burns, Lynch, Cosby, Fenn, & Baron, 2011). These decreases in S deposition and soil acidification are beginning to show signs of recovery in some areas (Hazlett et al., 2020; Gregory B Lawrence & Bailey, 2021; Gregory B. Lawrence et al., 2015), though full recovery could still take decades (Hazlett et al., 2020). A detailed dendroisotopic analysis for *Juniperus virginiana* (eastern red cedar) in the Central Appalachians found striking recovery beginning around 1982, with increases in stomatal conductance, photosynthesis, and growth that was mostly related to reductions in S emissions and to a lesser extent rising CO_2 (R. B. Thomas, Spal, Smith, & Nippert, 2013). Our study also finds that the growth and survival of *Juniperus virginiana* is reduced with S deposition (C. M. Clark et al., 2021; Horn et al., 2018), and thus that decreases in S deposition would increase growth (Table S2: +21.1%, Fig. 3). Similar increases have been reported for *Picea rubens* (red spruce) recovering from acid deposition (Mathias & Thomas, 2018), which also was predicted to increase with reductions in S deposition in our simulations (Table S2, +7.5%).

Reduced N fertilization could come with benefits, as pest outbreaks on tissue rich N could be reduced (L.H. Pardo et al., 2011; Stanke et al., 2021), and the potential for increased risk of hydraulic failure under drought could be mitigated (Fan et al., 2022; Gessler et al., 2017). It is difficult to compare our results with the many N fertilization studies that have been conducted because rates of N fertilization are often much higher than N deposition, and previous work suggests the tree growth and survival responses to N are non-linear (Canham & Murphy, 2016, 2017; Horn et al., 2018). Nonetheless, there are a handful of low N addition studies that we may compare our results with (reviewed in (Gilliam, Goodale, Pardo, Geiser, & Lilleskov, 2011)). Research in a red pine plantation (*Pinus resinosa*) in Harvard Forest, Massachusetts, examined the effect of N addition of 50 kg N ha-1 yr-1 on top of 9 kg N ha-1 yr-1 of deposition (Magill et al., 2004). They found N addition led to a decrease in tree growth and in increase in mortality (Magill et al., 2004). Red pine survival and growth increased at low rates of N deposition in our earlier study (Horn et al., 2018), but peaked at roughly 7 and 30 kg N ha-1 yr-1, respectively, decreasing at higher N deposition rates. Thus, total N inputs at 59 kg N ha-1 yr-1 could lead to reductions in growth and survival as found in (Magill et al., 2004), which is not inconsistent with our findings. Our results were more equivocal in comparison with results from the same research site for a mixed hardwood stand that was predominantly black oak and red maple (Magill et al., 2004). Growth was not reported by species, but researchers found no effect on total woody biomass for the low N addition rate of 50 kg N ha-1 yr-1. We found in (Horn et al., 2018) that growth of both species increased with N deposition. For survival, N fertilization in Magill et al. (2004) led to a small decrease for black oak (−4.6%) and a larger decrease for red maple (−6.8%). This is not inconsistent with our results from (Horn et al., 2018),

as we found a decrease in survival for red maple and no effect on black oak but for much lower N deposition levels (4–24 kg N ha-1 yr-1, versus a total input of 59 kg N ha-1 yr-1 in (Magill et al., 2004)).

An earlier related study for the Northeast also found a fertilization effect from N with wide variation in species relative abundances from changes in climate change and N deposition into the future (Van Houtven et al., 2019). However, that study was based on tree species growth and survival responses to N deposition from the 1980s-90s and was restricted to the mid-Atlantic and Northeastern United States (R. Q. Thomas, Canham, Weathers, & Goodale, 2010). Follow up work has since reported that species relationships have changed over time (C. M. T. Clark, R Quinn; Horn, Kevin J, 2023; Horn et al., 2018). Indeed, Clark et al. (2023) found that the growth or survival relationship with N had become more negative for 11 species, and more positive for five species. Thus, shifts towards more negative relationships with N in the eastern U.S. have occurred despite reductions in N deposition (Lloret & Valiela, 2016; Zhang et al., 2019). Soil recovery in the eastern U.S. appears to be beginning (Gregory B. Lawrence et al., 2015), even though legacy effects from prior N and S deposition appear to remain. Studies from Europe suggest recovery following reductions in N and S deposition (Boxman et al., 1998) that may be heterogenous among sites (Boxman et al., 1998; Hazlett et al., 2020). Multi-temporal analyses on the full panel of FIA data in the U.S. would shed additional light on the shifting responses among regions and species through time. Only in the past few years have enough of the FIA plots been sampled more than three times to enable such a multi-period examination.

Effects from climate change

Despite these projected benefits from reduced N and S deposition, we find that negative effects from future projected increases in MAT may ultimately overwhelm these benefits for the majority of tree species. These results generally agree with the recent literature that often focuses on fewer species or on forest types. In an experimental study on juvenile trees, Reich et al. (2022) found that increases in temperature (+1.6 C and +3.1 C) comparable to our $C_{4.5}$ simulations (Fig. 1, +2 C) led to increased growth for *Acer rubrum* and *Acer saccharum* and decreased growth for *Abies balsamea*, *Picea glauca* and *Pinus strobus*. Our results generally agree, with the $C_{4.5}$ scenario predicting an increase in *Acer rubrum* (1.5%) and *Acer saccharum* (7.7%), and a decrease in *Abies balsamea* (−10.2%) and *Picea glauca* (−16.9%) (Table S2). We are uncertain why our results agree for these four species but not for *Pinus strobus*, which we found would increase under the $C_{4.5}$ scenario (+4.8%, Table S2). An analysis across Canada's boreal forests found a strong negative effect on growth from temperature and positive effect from soil moisture (Girardin et al., 2016). Of the 1,119 global change experiments reviewed in (Song et al., 2019), less than 1% examined the effects of warming and nitrogen, and most of those were not on forests or trees. More research is clearly needed in these areas. An observational study in the western U.S. that also used the FIA data (Stanke et al., 2021), found that *Pseudotsuga menziesii* and *Pinus ponderosa* were increasing while *Abies lasiocarpa*, *Populus tremuloides*, *Picea engelmannii*, and *Pinus contorta* were decreasing. Direct comparisons with Stanke et al. (2022) are difficult as the measures of abundance are very different between the studies, but we also found *Pseudotsuga menziesii* and *Pinus ponderosa* were projected to increase mostly

from positive effects of increases in temperature (+9.5% and +9.6%, respectively, for $C_{4.5}$ scenario, Table S2).

Importantly, our study does not account for the potential for elevated CO_2 to stimulate tree growth, improve water use efficiency, and potentially offset the decreases projected here (Chen, Riley, Prentice, & Keenan, 2022; E. C. Davis, Sohngen, & Lewis, 2022; Song et al., 2019). However, it was not possible to incorporate the CO_2 fertilization directly in our analytical architecture given the spatial differences in CO_2 are small and the full panel of FIA plots have only been resampled in the past 20 years or so. Furthermore, the strength and longevity of the CO_2 fertilization effect is still uncertain and actively debated. A global tree ring study found limited evidence for CO_2 fertilization, with only 20 percent of sites globally exhibiting increasing trends in growth that could not be attributed to other factors (Gedalof & Berg, 2010). The aforementioned analysis across the boreal forests of Canada found no positive effect of CO_2 fertilization since 1950 (Girardin et al., 2016). Thus, although the CO_2 fertilization effect is commonly detected among manipulative studies that often examine higher CO_2 rates and younger trees (R. J. Norby et al., 2005; Song et al., 2019), its effect at the forest level is likely contingent on other factors such as mycorrhizal association, soil moisture, and nutrient limitation from N or P (Girardin et al., 2016; Goswami et al., 2018; Luo et al., 2004; Nate G McDowell et al., 2020; Terrer et al., 2016).

Higher temperatures in our study are a surrogate for many mechanisms that affect trees, including water stress, reduced photosynthesis from closed stomata, and higher mortality rates (Nate G McDowell et al., 2020; Park et al., 2013; Reich et al., 2022). Other climate-related effects not captured in our study also impact tree species, such as effects from wildfire (increase in fire intensity and fire occurrence), pathogens, extreme weather events, and others, which could compound effects reported here (Nate G McDowell et al., 2020; Vose, 2018). Our study is not intended to be a mechanistic examination of the processes by which these many factors interact to affect tree growth and survival. More detailed physiological and experimental work is needed for that (e.g., (Reich et al., 2022; R. B. Thomas et al., 2013)) which is not feasible to do for all 94 species presented here. Nonetheless, we are initiating follow up work to add more complexity to these models. In our study temperature, precipitation and N and S deposition are integrating variables that may affect tree species through a variety of positive and negative pathways, but that integrate to the whole tree growth and survival as reported here and in the foundational response curves here and elsewhere (Canham & Murphy, 2016, 2017; Horn et al., 2018; R. Q. Thomas et al., 2010). Future work is needed to incorporate these factors into the foundational response curves to update the response curves used in this study.

Additional considerations: Scale and limits in the observational record

It is important to highlight that the projected spatial differences among counties (i.e., Fig. 5) may be modest, but these modest effects accumulate across a species' range into a large effect (e.g., Fig. 3). These small effects over a wider area may even exceed in total those of large events like wildfires and pest outbreaks, provided that the forests recover. For example, data from the National Interagency Coordination Center (NICC) on Wildland Fire

shows that large wildfire years tend to lead to roughly 10 million acres burned (CRS, 2022). These are catastrophic events that affect forests and the nearby wildland-human interface, destroying property and killing trees in an area. However, 10 million acres represents only 5% of the National Forest System and 2.4% of the lands covered in forest in the CONUS in 2020. There were only 2 out of 94 species we examined that were relatively unaffected (<5%) by all scenarios examined here (*Thuja plicata, Abies concolor*) which suggests that probably all of the roughly 400 million acres of the forested acres in CONUS are affected by one or more of the drivers examined here. Thus, an important question emerges – what level of subtle effect, if widespread enough, is comparable in scale to the effects from larger events like wildfire and pest outbreaks? These larger events are critical to understand, especially given that they may lead to wholesale conversion of forested areas to non-forested. But, their effects may actually be much smaller overall than these subtle but pervasive effects on forest composition.

It is also important to acknowledge that many of these species may be pushed beyond the limits of the empirical record in our simulations. Growth and survival responses outside the empirical range of data are highly uncertain, and could be subject to thresholds that we have no data with which to detect. We did not extrapolate the growth or survival response curves beyond the observed deposition (2000–2014) or climate (2000–2016) ranges used in their original derivation (Horn et al., 2018) because we felt it inappropriate to extend the curves into areas with no observed responses. Instead, we flagged these trees as uncertain, and pinned the value at the maximum or minimum value, respectively, if the driver (e.g., temperature) went above or below the range of the observed record. For MAP, this did not introduce significant uncertainty, while for N deposition, S deposition, and MAT it may have. For MAP, none of the scenarios flagged more than 1% of trees (Table S3). N and S deposition was projected to go below the observed range for roughly 10% of trees for N and 40% of trees for S (Table S3). For reductions in N this occurred in pockets in the East and West, while for S this was throughout the eastern half of U.S. (Fig. 6a and 6b). Moving below the minimum N or S deposition may not be concerning since reductions in either are generally considered beneficial as this represents returning to a less polluted state. For temperature, the effects depended strongly on which RCP scenario was examined. Increased temperatures in the RCP 4.5 scenario only flagged roughly 1% of trees, mostly in the far south, southwest, and west coast (Fig. 6c). However, the RCP 8.5 scenarios flagged roughly 20% of trees throughout the CONUS (Table S2 and Fig. 6d and 6e). The underlying FIA database used here represents almost 100 billion U.S. trees sampled between 2000 and 2016, suggesting that roughly one billion (RCP 4.5) up to roughly 20 billion (RCP 8.5) trees are projected to experience temperatures warmer than the record used to derive these response curves by 2100. The experimental warming expiring conducted by Reich et al. (2022) found that effects were particularly negative when treatments simulated conditions warmer or drier than the historical range of conditions experienced (Reich et al., 2022). This observation combined with our results suggests severe implications for U.S. forests especially under the RCP 8.5 scenario. Flagged species under the $C_{8.5,wet}$ scenario were dominated by *Pinus taeda*, *Lithocarpus densiflorus*, *Picea mariana*, *Pseudotsuga menziesii*, and *Picea rubens* (all ≥ roughly 250 million trees flagged after expansion) while flagged species under the $C_{8.5,dry}$ were dominated by *Pinus taeda*, *Pseudotsuga menziesii*, *Tsuga*

heterophylla, *Lithocarpus densiflorus*, and *Juniperus osteosperma* (all ≥ roughly 250 million trees flagged after expansion). This is a significant risk at the high temperature range and suggest an urgent need to understand how trees may respond to these higher temperatures. Understanding the effects of increases in MAT above the empirically observed ranges, as well as effects of more extreme episodic events at these higher means, is critical to anticipating the effects of future changes in climate (Vose, 2018).

Uncertainties and Limitations

It is important to note that simple narratives, though convenient for the public and for communication purposes, may not be scientifically accurate. There are "winners and losers" across the spectrum of scenarios explored here, with many species benefitting or harmed, for all drivers examined. We do not yet understand what drives this variation in response. Phylogeny does not appear to be a major driver, as there were closely related species at both extremes of the climate effects (e.g., *Pinus banksiana* vs. *Pinus contorta* [−74% vs. +78%, average climate effects], *Quercus veluntina* vs. *Quercus ellipsoidalis* [−59% vs. +58%], Fig. 4, Table S2). There are many factors that could contribute in addition to phylogeny, including ambient edaphic conditions (Hazlett et al., 2020), climate conditions (Nate G McDowell et al., 2020), mycorrhizal symbioses (Averill, Dietze, & Bhatnagar, 2018), and others (Carter et al., 2017). Disaggregating effects to the species level enhances our basic understanding of forest responses, though it also complicates communication of those findings to the public and to policymakers. Furthermore, most of the species reported here have little or no experimental studies with which to compare. Experimental studies – for good reason - often focus on only a handful of common species within a site or region rather than assessing the responses across the full community. Future modeling under the IPCC may benefit from revising representations of simplified forest types (e.g., deciduous broadleaf, etc., (Wieder, Cleveland, Smith, & Todd-Brown, 2015)) by aggregating species-level empirical responses presented here and elsewhere into those forest types, and/or by introducing stochasticity of forest responses though variation among species within a forest type.

There are several specific limitations to this study that deserve discussion. These can be binned for convenience into either those related to the underlying response curves from Horn et al. (2018), and those related to their application in the forest model here. Related to the response curves, there are several factors that affect tree growth and survival that were not included in Horn et al. (2018), including CO_2, wildfire, pest pressures, stand development, forest management and many others. Because they were not included in the original derivation of the species curves, they were not used in the simulations of future impacts because we had no way to estimate their effects for each species examined. Thus, the estimates here represent projected changes in forest composition assuming those other factors are held constant or offset. Recent findings in (E. C. Davis et al., 2022) suggest many of the species here respond positively to CO_2. However, no effects from CO_2 on tree growth have been reported in other studies (Gedalof & Berg, 2010; Girardin et al., 2016), suggesting there is still work to be done in this area. This effort is not intended to be an analysis of all factors affecting trees, but rather to be a comprehensive examination from four factors known to be important, using a common methodology to facilitate comparisons among

species of relative vulnerability. That said, expanding the foundational response curves to capture more drivers is an urgent need. Finally, there are no interactions in these models (Horn et al., 2018), these are multiplicative terms with independently estimated statistical terms. The derivation of the response curves in Horn et al. (2018) was computationally intensive, requiring several months runtime on a supercomputer. Thus, new approaches that are more computationally efficient (e.g., Machine Learning, (Pavlovic et al., 2023)) and or new data processing techniques may need to be developed to add more factors, species, and complex interactions.

The forest model we used also has important limitations. Primary among those is there is no recruitment of new individuals. Thus, our estimates represent changes to the 2000–2016 cohort of mixed-species and -age trees. Further into the future, the current cohort will comprise a smaller and smaller fraction of the forest. Future work will need to be conducted to develop similar response curves for seedlings and saplings to enable multi-cohort estimates. Similar research has been conducted for the growth and survival of saplings in the eastern U.S. (Canham & Murphy, 2016, 2017), but no work to our knowledge has tied this to recruitment of new adult trees. This may be challenging, as the FIA often does not distinguish these smaller individuals to the species level as identification is more difficult. Because there is no recruitment, there is also no migration, as migration is the movement of new individuals to new areas. Solutions to both challenges are being developed. In addition to this limitation, our model runs are bounded by the observed range of data and conditions for 2000–2016 (Horn et al., 2018). We have no reason to expect this period to be anomalous, but the observed record is not wide enough to enable confident projections of what may happen at the low end of N and S deposition or at higher temperatures across all scenarios. The former is not anticipated to be problematic, while the latter may be alarming. We could have extended the curves in Horn et al. (2018) beyond the empirical record in our model, but there may be important tipping points in those regions that we are unaware of and we felt it more appropriate to flag these trees and constrain our estimates to the empirical record. More detailed examination of tree responses at these higher mean annual temperatures would improve our understanding of how forests and tree species may be affected in the future. In addition, many U.S. tree species were omitted in Horn et al. (2018). Although the majority of the forest basal area for most of the CONUS is captured by the 94 species included (Fig. S1), there are many regionally important species not captured, including *Pinus albicaulis* (whitebark pine, recently listed as endangered due in part to climate change, (FWS, 2022)), *Sequoia sempervirens* (Redwood), and *Sequoiadendron giganteum* (Giant Sequoia). Follow on work will focus on incorporation of more species. Finally, we also don't incorporate changes in forest acreage or management over the simulation period, which are very difficult to predict.

Notwithstanding these important areas of future improvement, these results represent our best available projections for how the current cohort, representing nearly 90 billion trees across the CONUS, are anticipated to respond to changes in MAT, MAP, and reductions in N and S deposition to the end of century.

Conclusions

Overall, we find that negative effects from future projected increases in mean annual temperature may ultimately overwhelm positive effects from reductions in N and S deposition for the majority of tree species. This study highlights that changes in forest growth and survival rates at the species level are expected to shift community composition in the future. These shifts, though subtle for a particular place, may be dramatic for many species presenting challenges to networks monitoring forest health, and suggesting additional research areas for the future.

Supplementary Material

Refer to Web version on PubMed Central for supplementary material.

Acknowledgements

The views expressed here are those of the authors and do not necessarily represent the views or policies of the U.S. Environmental Protection Agency or any other agency of the U.S. government. This work was supported under contracts EP-C-11–036 and EP-W-11–029. We thank Steve Leduc and Jason Lynch for helpful reviews of earlier drafts of the manuscript. The authors declare no competing interests.

Data Availability:

Data are available on Dryad at https://doi.org/10.5061/dryad.tht76hf4f.

References

Aber J, McDowell W, Nadelhoffer K, Magill A, Berntson G, Kamakea M, . . . Fernandez I. (1998). Nitrogen saturation in temperate forest ecosystems - Hypotheses revisited. BioScience, 48(11), 921–934. Retrieved from <Go to ISI>://000076533500009

Averill C, Dietze MC, & Bhatnagar JM (2018). Continental-scale nitrogen pollution is shifting forest mycorrhizal associations and soil carbon stocks. Global Change Biology, 24(10), 4544–4553. [PubMed: 30051940]

Bobbink R, Hicks K, Galloway J, Spranger T, Alkemade R, Ashmore M, . . . De Vries W. (2010). Global assessment of nitrogen deposition effects on terrestrial plant diversity: a synthesis. Ecological Applications, 20(1), 30–59. Retrieved from <Go to ISI>://000275358100004 [PubMed: 20349829]

Boxman AW, Blanck K, Brandrud T-E, Emmett BA, Gundersen P, Hogervorst RF, . . . Timmermann V. (1998). Vegetation and soil biota response to experimentally-changed nitrogen inputs in coniferous forest ecosystems of the NITREX project. Forest Ecology And Management, 101(1–3), 65–79.

Burnham K. a. D. A. (2002). Model Selection and Multimodel inference: Springer.

Burns DA, Lynch JA, Cosby BJ, Fenn ME, & Baron JS (2011). National Acid Precipitation Assessment Program Report to Congress 2011: An Integrated Assessment. Retrieved from Washington, DC:

Cabon A, Kannenberg SA, Arain A, Babst F, Baldocchi D, Belmecheri S, . . . McKenzie S. (2022). Cross-biome synthesis of source versus sink limits to tree growth. Science, 376(6594), 758–761. [PubMed: 35549405]

Campbell PC, Bash JO, Nolte CG, Spero TL, Cooter EJ, Hinson K, & Linker L. (2019). Projections of atmospheric nitrogen deposition to the Chesapeake Bay watershed. J. Geophys. Res. Biogeosci., 12(11), 3307–3326. doi:10.1029/2019JG005203 [PubMed: 33868882]

Canham CD, & Murphy L. (2016). The demography of tree species response to climate: sapling and canopy tree growth. Ecosphere, 7(10), e01474.

Canham CD, & Murphy L. (2017). The demography of tree species response to climate: sapling and canopy tree survival. Ecosphere, 8(2), e01701.

Carter TS, Clark CM, Fenn ME, Jovan S, Perakis SS, Riddell J, . . . Hastings MG (2017). Mechanisms of nitrogen deposition effects on temperate forest lichens and trees. Ecosphere, 8(3):e01717.10.1002/ecs2.1717.

Chen C, Riley WJ, Prentice IC, & Keenan TF (2022). CO2 fertilization of terrestrial photosynthesis inferred from site to global scales. Proceedings of the National Academy of Sciences, 119(10), e2115627119.

Clark CM, Sabo R, Geiser L, Perakis SP, Schaberg PG, & [eds.]. (2021). Air pollution effects on forests: A guide to species ecology, responses to nitrogen and sulfur deposition, and associated ecosystem services. Vol I. Trees. FS-1156. Washington, DC: U.S. Department of Agriculture, Forest Service. 206 p. Vol. 1.

Clark CMT, Quinn R; Horn, Kevin J. (2023). Above-ground tree carbon storage in response to nitrogen deposition in the U.S. is heterogeneous and may have weakened. Communications Earth and Environment, accepted. DOI: 10.1038/s43247-023-00677-w.

Cronan CS, April R, Bartlett RJ, Bloom PR, Driscoll CT, Gherini SA, . . . Parnell RA (1989). Aluminum toxicity in forests exposed to acidic deposition: the ALBIOS results. Water, Air, and Soil Pollution, 48, 181–192.

CRS. (2022). Congressional Research Service (CRS). Wildfire Statistics. Data from the NICC Wildland Fire Summary and Statistics annual reports. https://sgp.fas.org/crs/misc/IF10244.pdf.

Daly C, Halbleib M, Smith JI, Gibson WP, Doggett MK, Taylor GH, . . . Pasteris PP (2008). Physiographically sensitive mapping of climatological temperature and precipitation across the conterminous United States. International Journal of Climatology, 28(15), 2031–2064.

Davis EC, Sohngen B, & Lewis DJ (2022). The effect of carbon fertilization on naturally regenerated and planted US forests. Nature communications, 13(1), 5490.

Davis KT, Dobrowski SZ, Higuera PE, Holden ZA, Veblen TT, Rother MT, . . . Maneta MP (2019). Wildfires and climate change push low-elevation forests across a critical climate threshold for tree regeneration. Proceedings of the National Academy of Sciences, 116(13), 6193–6198.

Dietze MC, & Moorcroft PR (2011). Tree mortality in the eastern and central United States: patterns and drivers. Global Change Biology, 17(11), 3312–3326.

EPA. (2013a). Air quality modeling technical support document: proposed Tier 3 emission standards. Air Quality Assessment Division Office of Air Quality Planning & Standards U.S. Environmental Protection Agency. EPA-454/R-13–006. Available at: http://www.epa.gov/otaq/documents/tier3/454r13006.pdf. Accessed on 08/12/2015.

EPA. (2013b). Draft regulatory impact analysis: Tier 3 motor vehicle emission & fuel standards. Air Quality Assessment Division Office of Air Quality Planning & Standards U.S. Environmental Protection Agency. EPA-420-D-13–002. Available at:http://www.epa.gov/otaq/documents/tier3/420d13002.pdf. Accessed on 08/12/2015.

EPA. (2020). U.S. EPA. Integrated Science Assessment (ISA) for Oxides of Nitrogen, Oxides of Sulfur and Particulate Matter Ecological Criteria (Final Report, 2020). U.S. Environmental Protection Agency, Washington, DC, EPA/600/R-20/278, 2020.

EPA. (2023). Climate Change Indicators in the United States. https://www.epa.gov/climate-indicators.

Fan D-Y, Dang Q-L, Yang X-F, Liu X-M, Wang J-Y, & Zhang S-R (2022). Nitrogen deposition increases xylem hydraulic sensitivity but decreases stomatal sensitivity to water potential in two temperate deciduous tree species. Science Of The Total Environment, 848, 157840.

Fenn ME, Baron JS, Allen EB, Rueth HM, Nydick KR, Geiser L, . . . Neitlich P. (2003). Ecological effects of nitrogen deposition in the western United States. BioScience, 53(4), 404–420.

Fenn ME, Preisler HK, Fried JS, Bytnerowicz A, Schilling SL, Jovan S, & Kuegler O. (2020). Evaluating the effects of nitrogen and sulfur deposition and ozone on tree growth and mortality in California using a spatially comprehensive forest inventory. Forest Ecology And Management, 465, 118084.

FWS. (2022). Endangered and Threatened Wildlife and Plants; Threatened Species Status With Section 4(d) Rule for Whitebark Pine (Pinus albicaulis). 87 FR 76882. Docket No. FWS-R6-ES-2019–0054. https://www.federalregister.gov/d/2022-27087. December 15, 2022.

Galloway JN, Dentener FJ, Capone DG, Boyer EW, Howarth RW, Seitzinger SP, . . . Vorosmarty CJ (2004). Nitrogen cycles: past, present, and future. Biogeochemistry, 70(2), 153–226. Retrieved from <Go to ISI>://000226518900001

Gedalof Z. e., & Berg AA (2010). Tree ring evidence for limited direct CO2 fertilization of forests over the 20th century. Global Biogeochem. Cyc, 24(3).

Gessler A, Schaub M, & McDowell NG (2017). The role of nutrients in drought-induced tree mortality and recovery. New Phytologist, 214(2), 513–520. [PubMed: 27891619]

Gilliam FS, Goodale CL, Pardo LH, Geiser LH, & Lilleskov EA (2011). Chapter 10: Eastern Temperate Forests. In Pardo LH, Robin-Abbott MJ and Driscoll CT, 2011. Assessment of nitrogen deposition effects and empirical critical loads of nitrogen for ecoregions of the United States. Gen. Tech. Rep. NRS-80. .

Girardin MP, Bouriaud O, Hogg EH, Kurz W, Zimmermann NE, Metsaranta JM, . . . Büntgen U. (2016). No growth stimulation of Canada's boreal forest under half-century of combined warming and CO2 fertilization. Proceedings of the National Academy of Sciences, 113(52), E8406–E8414.

Goswami S, Fisk MC, Vadeboncoeur MA, Garrison-Johnston M, Yanai RD, & Fahey TJ (2018). Phosphorus limitation of aboveground production in northern hardwood forests. Ecology, 99(2), 438–449. [PubMed: 29205288]

Grossiord C, Buckley TN, Cernusak LA, Novick KA, Poulter B, Siegwolf RT, . . . McDowell NG (2020). Plant responses to rising vapor pressure deficit. New Phytologist, 226(6), 1550–1566. [PubMed: 32064613]

Hazlett P, Emilson C, Lawrence G, Fernandez I, Ouimet R, & Bailey S. (2020). Reversal of forest soil acidification in the northeastern United States and eastern Canada: Site and soil factors contributing to recovery. Soil Systems, 4(3), 54.

Hicke JA, Meddens AJ, & Kolden CA (2016). Recent tree mortality in the western United States from bark beetles and forest fires. Forest Science, 62(2), 141–153.

Holland EA, Dentener FJ, Braswell BH, & Sulzman JM (1999). Contemporary and pre-industrial global reactive nitrogen budgets. In New Perspectives on Nitrogen Cycling in the Temperate and Tropical Americas (pp. 7–43): Springer.

Horn KJ, Thomas RQ, Clark CM, Pardo LH, Fenn ME, Lawrence GB, . . . Braun S. (2018). Growth and survival relationships of 71 tree species with nitrogen and sulfur deposition across the conterminous US. Plos One, 13(10), e0205296.

Jenkins JC, Chojnacky DC, Heath LS, & Birdsey RA (2003). National-scale biomass estimators for United States tree species. Forest science, 49(1), 12–35.

Lamarque JF, Bond TC, Eyring V, Granier C, Heil A, Klimont Z, . . . van Vuuren DP (2010). Historical (1850–2000) gridded anthropogenic and biomass burning emissions of reactive gases and aerosols: methodology and application. Atmospheric Chemistry and Physics, 10(15), 7017–7039. doi:10.5194/acp-10-7017-2010

Lawrence GB, & Bailey SW (2021). Recovery Processes of Acidic Soils Experiencing Decreased Acidic Deposition. In (Vol. 5, pp. 36): MDPI.

Lawrence GB, Hazlett PW, Fernandez IJ, Ouimet R, Bailey SW, Shortle WC, . . . Antidormi MR (2015). Declining Acidic Deposition Begins Reversal of Forest-Soil Acidification in the Northeastern U.S. and Eastern Canada. Environmental Science & Technology, 49(22), 13103–13111. doi:10.1021/acs.est.5b02904 [PubMed: 26495963]

LeBauer DS, & Treseder KK (2008). Nitrogen limitation of net primary productivity in terrestrial ecosystems is globally distributed. Ecology, 89(2), 371–379. doi:10.1890/06-2057.1 [PubMed: 18409427]

LeDuc SD, Clark CM, Phelan J, Belyazid S, Bennett MG, Boaggio K, . . . Jones P. (2022). Nitrogen and Sulfur Deposition Reductions Projected to Partially Restore Forest Soil Conditions in the US Northeast, While Understory Composition Continues to Shift with Future Climate Change. Water, Air, & Soil Pollution, 233(9), 1–26. [PubMed: 36312741]

Li Y, Schichtel BA, Walker JT, Schwede DB, Chen X, Lehmann CMB, . . . Collett JL Jr. (2016). Increasing importance of deposition of reduced nitrogen in the United States. Proceedings of the National Academy of Sciences of the United States of America, 113(21), 5874–5879. doi:10.1073/pnas.1525736113 [PubMed: 27162336]

Lloret J, & Valiela I. (2016). Unprecedented decrease in deposition of nitrogen oxides over North America: the relative effects of emission controls and prevailing air-mass trajectories. Biogeochemistry, 129(1), 165–180. doi:10.1007/s10533-016-0225-5

Luo Y, Su B, Currie WS, Dukes JS, Finzi A, Hartwig U, . . . Field CB (2004). Progressive nitrogen limitation of ecosystem responses to rising atmospheric carbon dioxide. BioScience, 54(8), 731–739. Retrieved from <Go to ISI>://WOS:000223146000009

Magill AH, Aber JD, Currie WS, Nadelhoffer KJ, Martin ME, McDowell WH, . . . Steudler P. (2004). Ecosystem response to 15 years of chronic nitrogen additions at the Harvard Forest LTER, Massachusetts, USA. Forest Ecology And Management, 196(1), 7–28. doi:10.1016/j.foreco.2004.03.033

Mathias JM, & Thomas RB (2018). Disentangling the effects of acidic air pollution, atmospheric CO 2, and climate change on recent growth of red spruce trees in the Central Appalachian Mountains. Global Change Biology, 24(9), 3938–3953. [PubMed: 29781219]

McDowell NG, & Allen CD (2015). Darcy's law predicts widespread forest mortality under climate warming. Nature Climate Change, 5(7), 669–672.

McDowell NG, Allen CD, Anderson-Teixeira K, Aukema BH, Bond-Lamberty B, Chini L, . . . Hanbury-Brown A. (2020). Pervasive shifts in forest dynamics in a changing world. Science, 368(6494), eaaz9463.

Melillo JM, Butler S, Johnson J, Mohan J, Steudler P, Lux H, . . . Tang J. (2011). Soil warming, carbon-nitrogen interactions, and forest carbon budgets. Proceedings of the National Academy of Sciences of the United States of America, 108(23), 9508–9512. doi:10.1073/pnas.1018189108 [PubMed: 21606374]

Norby RJ, DeLucia EH, Gielen B, Calfapietra C, Giardina CP, King JS, . . . Oren R. (2005). Forest response to elevated CO2 is conserved across a broad range of productivity. Proceedings of the National Academy of Sciences of the United States of America, 102(50), 18052–18056. doi:10.1073/pnas.0509478102 [PubMed: 16330779]

Norby RJ, Hanson PJ, O'Neill EG, Tschaplinski TJ, Weltzin JF, Hansen RA, . . . Edwards NT (2002). Net primary productivity of a CO2-enriched deciduous forest and the implications for carbon storage. Ecological Applications, 12(5), 1261–1266.

O'Connell BM, Conkling BL, Wilson AM, Burrill EA, Turner JA, Pugh SA, & Menlove J. (2017). The Forest Inventory and Analysis Database: database description and user guide version 7.0 for Phase 2. Retrieved from Newtown Square, Pennsylvania, USA: https://www.fia.fs.fed.us/library/database-documentation/

Pardo LH, Fenn M, Goodale CL, Geiser LH, Driscoll CT, E. A., . . . Dennis RL (2011). Effects of nitrogen deposition and empirical nitrogen critical loads for ecoregions of the United States. Ecological Applications, 21(8), 3049–3082.

Pardo LH, Fenn ME, Goodale CL, Geiser LH, Driscoll CT, Allen EB, . . . Dennis RL (2011). Effects of nitrogen deposition and empirical nitrogen critical loads for ecoregions of the United States. Ecological Applications, 21(8), 3049–3082. Retrieved from <Go to ISI>://WOS:000299166300016

Park WA, Allen CD, Macalady AK, Griffin D, Woodhouse CA, Meko DM, . . . Grissino-Mayer HD (2013). Temperature as a potent driver of regional forest drought stress and tree mortality. Nature Climate Change, 3(3), 292–297.

Pavlovic NR, Chang SY, Huang J, Craig K, Clark C, Horn K, & Driscoll CT (2023). Empirical nitrogen and sulfur critical loads of US tree species and their uncertainties with machine learning. Science Of The Total Environment, 857, 159252. [PubMed: 36216054]

Phelan J, Belyazid S, Jones P, Cajka J, Buckley J, & Clark C. (2016). Assessing the Effects of Climate Change and Air Pollution on Soil Properties and Plant Diversity in Sugar Maple–Beech–Yellow Birch Hardwood Forests in the Northeastern United States: Model Simulations from 1900 to 2100. Water, Air, & Soil Pollution, 227(3), 1–30.

Pierce DW, Cayan DR, & Thrasher BL (2014). Statistical downscaling using localized constructed analogs (LOCA). Journal of Hydrometeorology, 15(6), 2558–2585.

Pukkala T, Lähde E, & Laiho O. (2009). Growth and yield models for uneven-sized forest stands in Finland. Forest Ecology and Management, 258(3), 207–216.

Reich PB, Bermudez R, Montgomery RA, Rich RL, Rice KE, Hobbie SE, & Stefanski A. (2022). Even modest climate change may lead to major transitions in boreal forests. Nature, 1–6.

Sabo RD, Clark CM, Bash J, Sobota D, Cooter E, Dobrowolski JP, . . . Morford SL (2019). Decadal shift in nitrogen inputs and fluxes across the contiguous United States: 2002–2012. Journal of Geophysical Research: Biogeosciences, 124(10), 3104–3124.

Schaberg PG, DeHayes DH, Hawley GJ, Murakami PF, Strimbeck GR, & McNulty SG (2002). Effects of chronic N fertilization on foliar membranes, cold tolerance, and carbon storage in montane red spruce. Canadian Journal of Forest Research-Revue Canadienne De Recherche Forestiere, 32(8), 1351–1359. doi:10.1139/x02-059

Schwede D, & Lear G. (2014). A novel hybrid approach for estimating total deposition in the United States. Atmospheric Enivironment, 92, 207–220.

Solberg S, Dobbertin M, Reinds GJ, Lange H, Andreassen K, Fernandez PG, . . . de Vries W. (2009). Analyses of the impact of changes in atmospheric deposition and climate on forest growth in European monitoring plots: a stand growth approach. Forest Ecology and Management, 258(8), 1735–1750.

Song J, Wan S, Piao S, Knapp AK, Classen AT, Vicca S, . . . Beier C. (2019). A meta-analysis of 1,119 manipulative experiments on terrestrial carbon-cycling responses to global change. Nature Ecology & Evolution, 3(9), 1309–1320. [PubMed: 31427733]

Stanke H, Finley AO, Domke GM, Weed AS, & MacFarlane DW (2021). Over half of western United States' most abundant tree species in decline. Nature communications, 12(1), 1–11.

Terrer C, Vicca S, Hungate BA, Phillips RP, & Prentice IC (2016). Mycorrhizal association as a primary control of the CO2 fertilization effect. Science, 353(6294), 72–74. [PubMed: 27365447]

Thomas RB, Spal SE, Smith KR, & Nippert JB (2013). Evidence of recovery of Juniperus virginiana trees from sulfur pollution after the Clean Air Act. Proceedings of the National Academy of Sciences, 110(38), 15319–15324.

Thomas RQ, Canham CD, Weathers KC, & Goodale CL (2010). Increased tree carbon storage in response to nitrogen deposition in the US. Nature Geoscience, 3(1), 13–17. doi:10.1038/ngeo721

USFS. (2018). The Forest Inventory and Analysis Database: Database Description and User Guide for Phase 2 (version 8.0). https://www.fia.fs.fed.us/library/database-documentation/current/ver80/FIADB%20User%20Guide%20P2_8-0.pdf.

USGCRP. (2017). Climate Science Special Report: Fourth National Climate Assessment, Volume I [Wuebbles DJ, Fahey DW, Hibbard KA, Dokken DJ, Stewart BC, and Maycock TK (eds.)]. U.S. Global Change Research Program, Washington, DC, USA, 470 pp., doi: 10.7930/J0J964J6.

Van Houtven G, Phelan J, Clark C, Sabo RD, Buckley J, Thomas RQ, . . . LeDuc SD (2019). Nitrogen deposition and climate change effects on tree species composition and ecosystem services for a forest cohort. Ecological Monographs, 89(2), e01345. doi:10.1002/ecm.1345

Vose, J. M. D. L. P. G. M. D. C. J. F. L. A. J. R. E. K. C. H. L. J. P. P. (2018). Forests. In Impacts, Risks, and Adaptation in the United States: Fourth National Climate Assessment, Volume II [Reidmiller DR, Avery CW, Easterling DR, Kunkel KE, Lewis KLM, Maycock TK, and Stewart BC (eds.)]. U.S. Global Change Research Program, Washington, DC, USA, pp. 232–267. doi: 10.7930/NCA4.2018.CH6.

Walker AP, De Kauwe MG, Medlyn BE, Zaehle S, Iversen CM, Asao S, . . . Hungate BA (2019). Decadal biomass increment in early secondary succession woody ecosystems is increased by CO2 enrichment. Nature Communications, 10(1), 1–13.

Wear DN, & Coulston JW (2015). From sink to source: Regional variation in US forest carbon futures. Scientific Reports, 5(1), 1–11.

Wieder WR, Cleveland CC, Smith WK, & Todd-Brown K. (2015). Future productivity and carbon storage limited by terrestrial nutrient availability. Nature Geoscience, 8(6), 441–444.

Zhang Y, Foley KM, Schwede DB, Bash JO, Pinto JP, & Dennis RL (2019). A measurement-model fusion approach for improved wet deposition maps and trends. J Geophys Res Atmos, 124(7), 4237–4251. doi:10.1029/2018JD029051 [PubMed: 31218153]

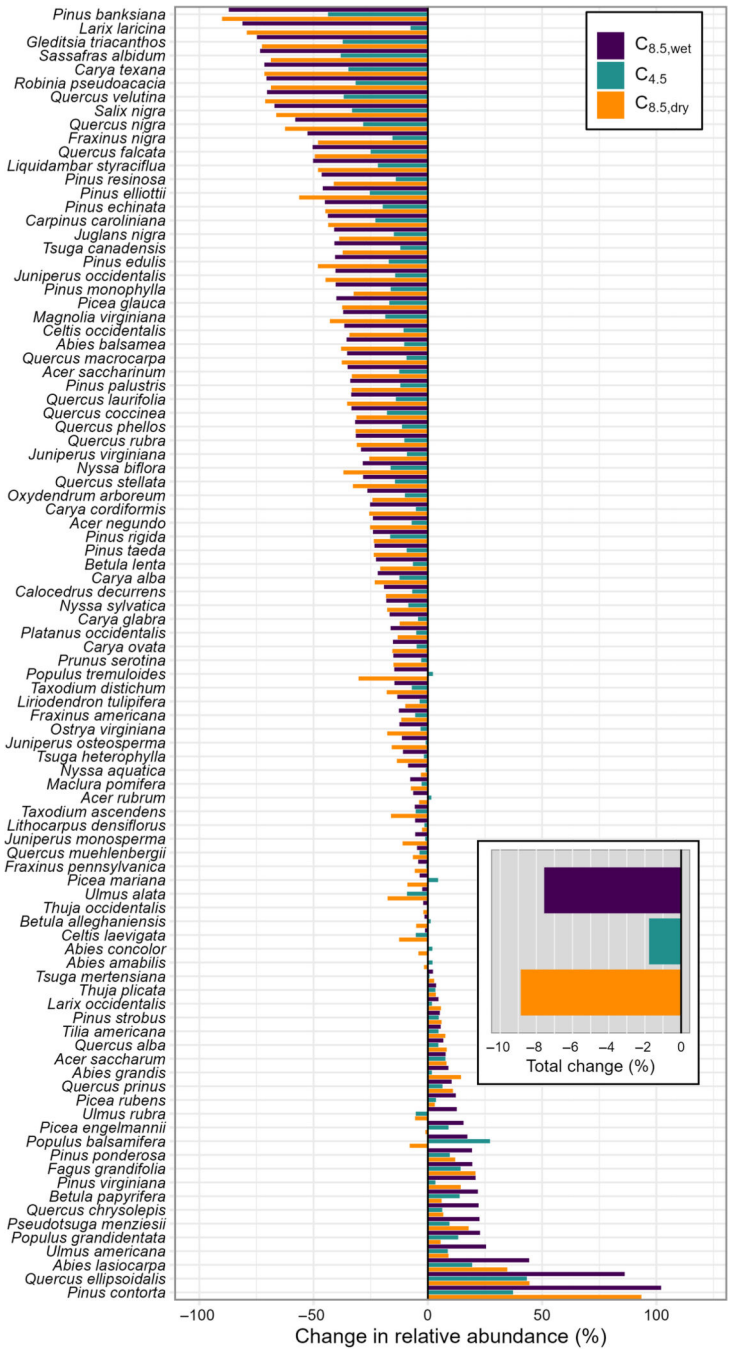

Fig. 1. The deposition and climate scenarios used in the study.

The table (left) describes the scenarios examined (all 20 combinations of climate and deposition scenarios were run). Hereafter, combined scenarios are listed together where appropriate (e.g., for current deposition and climate as D_0_CC). The deposition linear plot (top right) shows the scenarios of average CONUS deposition through time. The climate biplot (bottom right) summarizes the average CONUS changes between 2000–2020 and 2080–2100 for the scenarios explored here (points). For reference also shown are the range

from the full ensemble of IPCC AR5 models for RCP 4.5 (red polygon) and 8.5 (blue polygon).

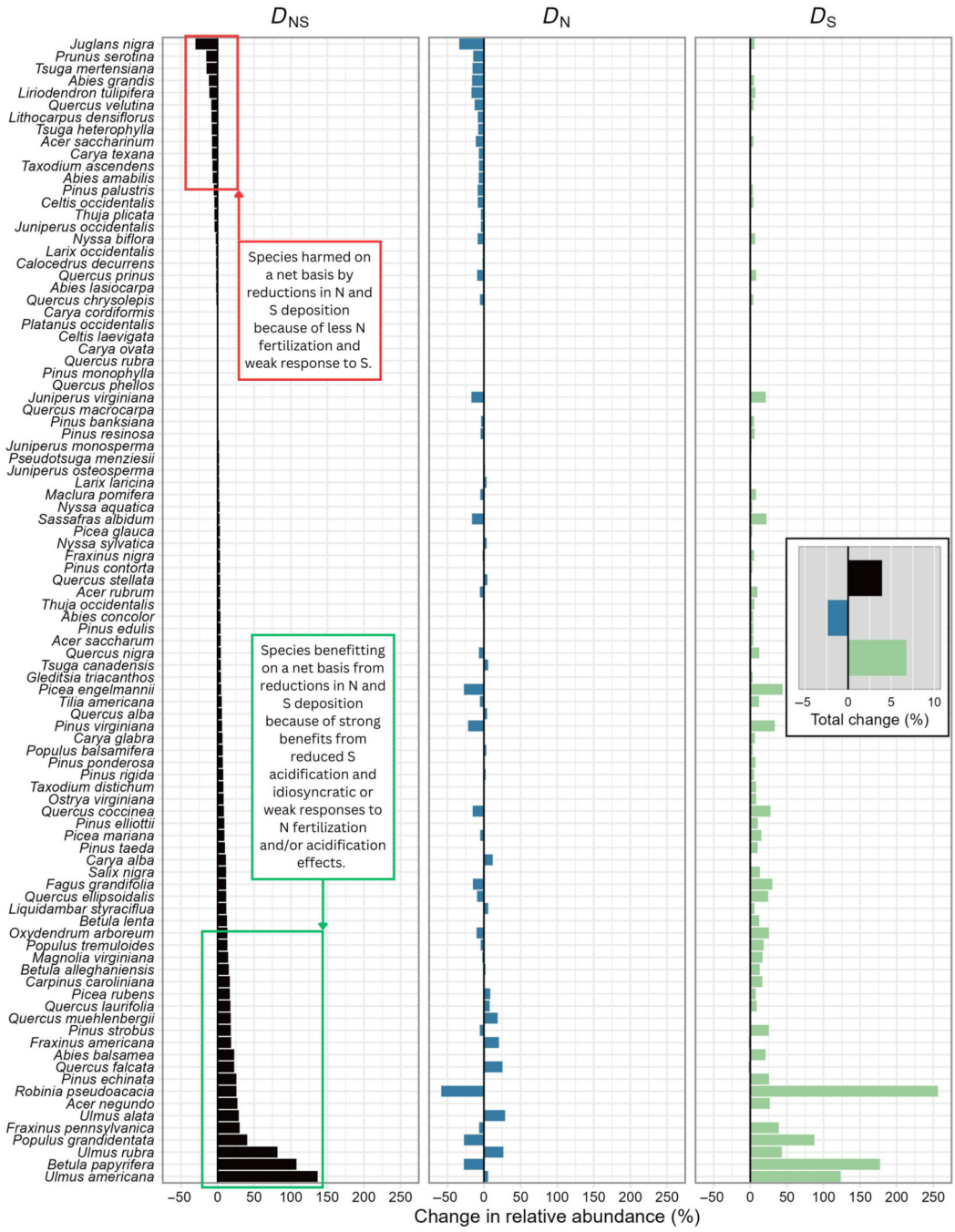

Fig. 2: Biomass of the cohort of trees in 2100 across all 20 scenarios.
See Fig. 1 for description of scenarios.

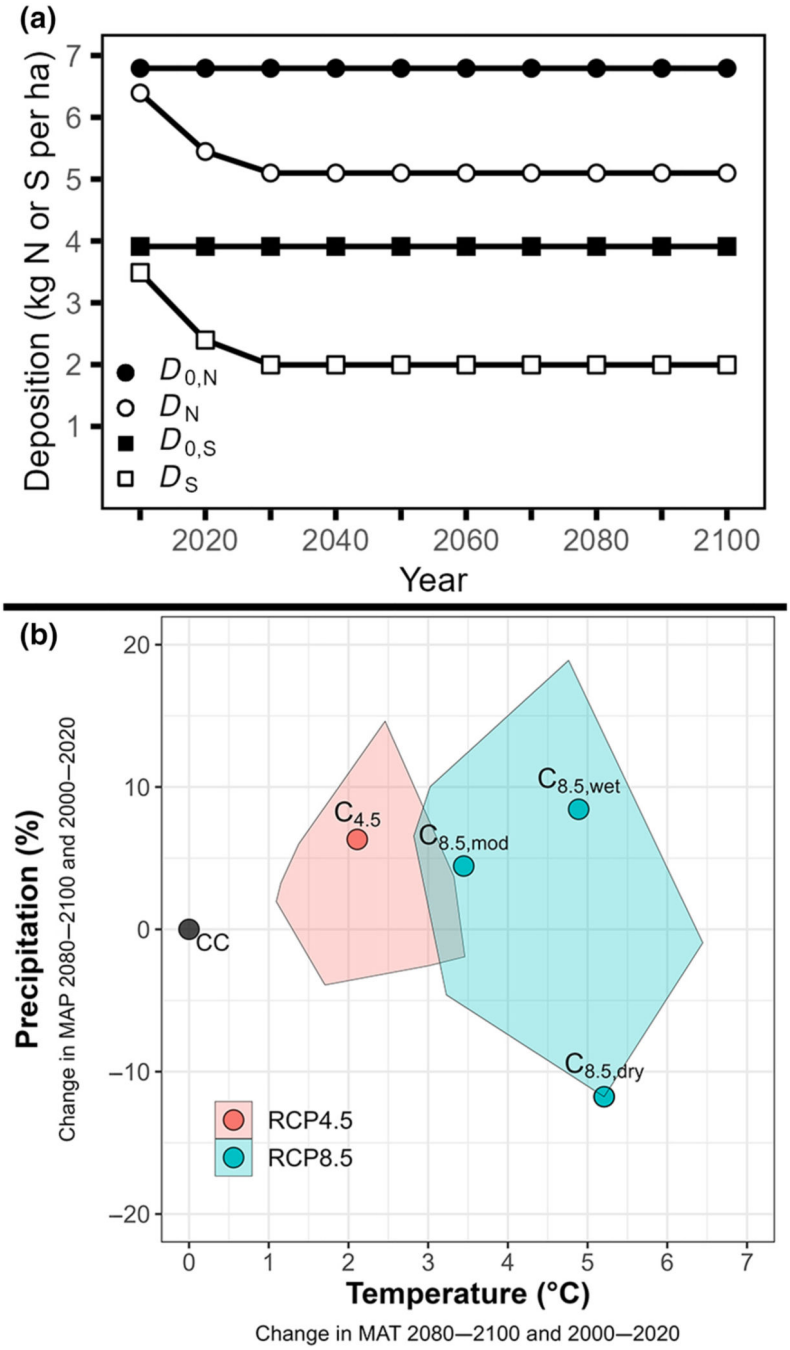

Fig. 3: Differences in relative abundance (%) in 2100 at the CONUS level for deposition scenarios.

Shown are differences for each of the 94 modeled tree species comparing D_{NS} with D_0 (a), D_N with D_0 (b), and D_S with D_0 (c). All comparisons used a constant climate. Changes for deposition scenarios are calculated as the relative difference in 2100 between the scenario with and without deposition reduction assuming a constant climate ordered by effect from N+S reduction (e.g., for 3a that is: (D_{NS}_CC – D_0_CC)/D_0_CC, see Table S2 for values).

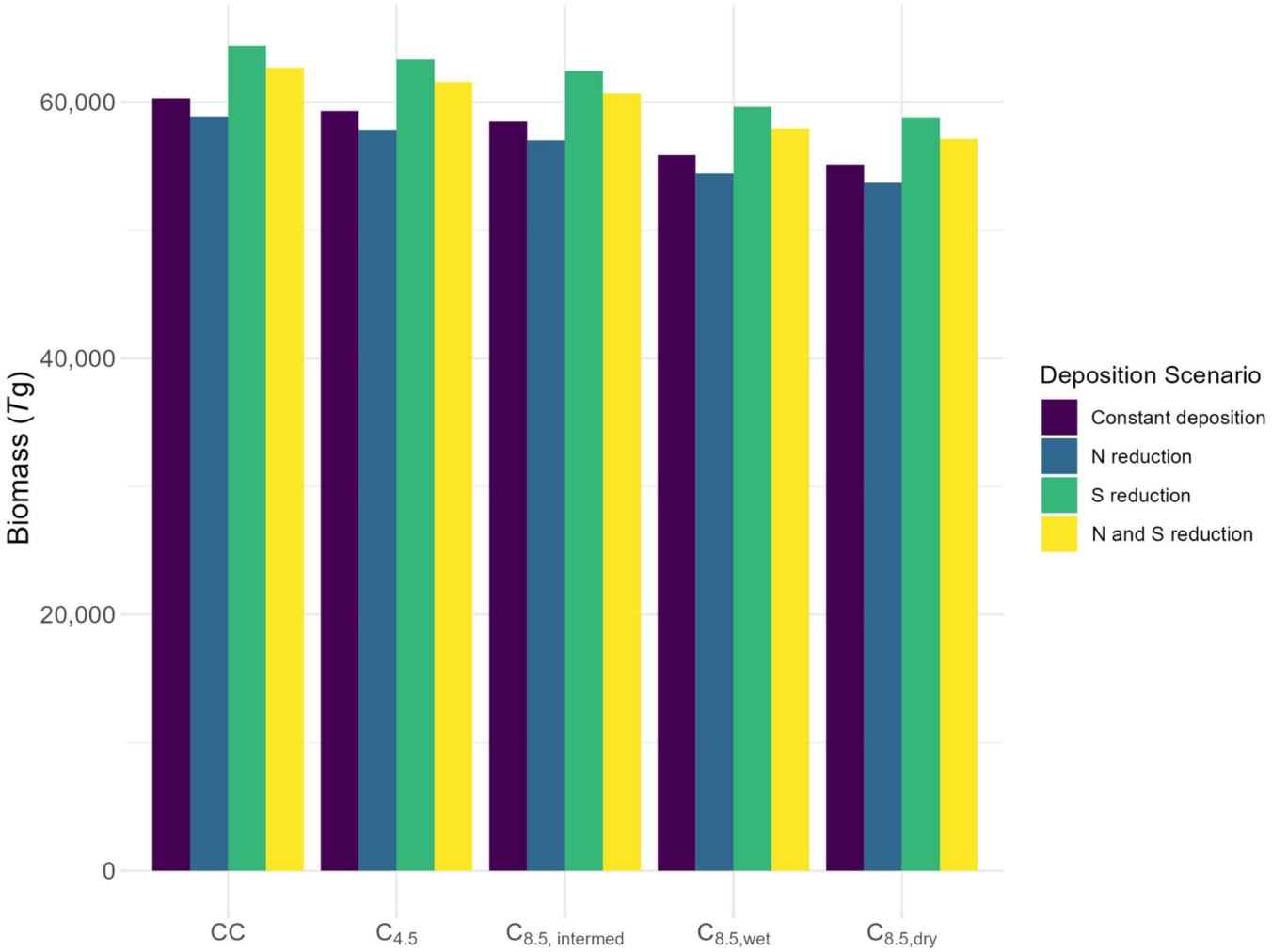

Fig. 4: Changes in relative abundance (%) in 2100 for climate scenarios.

Changes for climate scenarios are calculated as the relative difference between the scenario with and without climate change assuming reduced deposition (e.g., ($D_{NS\_}C_{8.5,dry}$ − $D_{NS\_}CC$)/ in Fig. 1). Ordered by $C_{8.5,wet}$ effect.

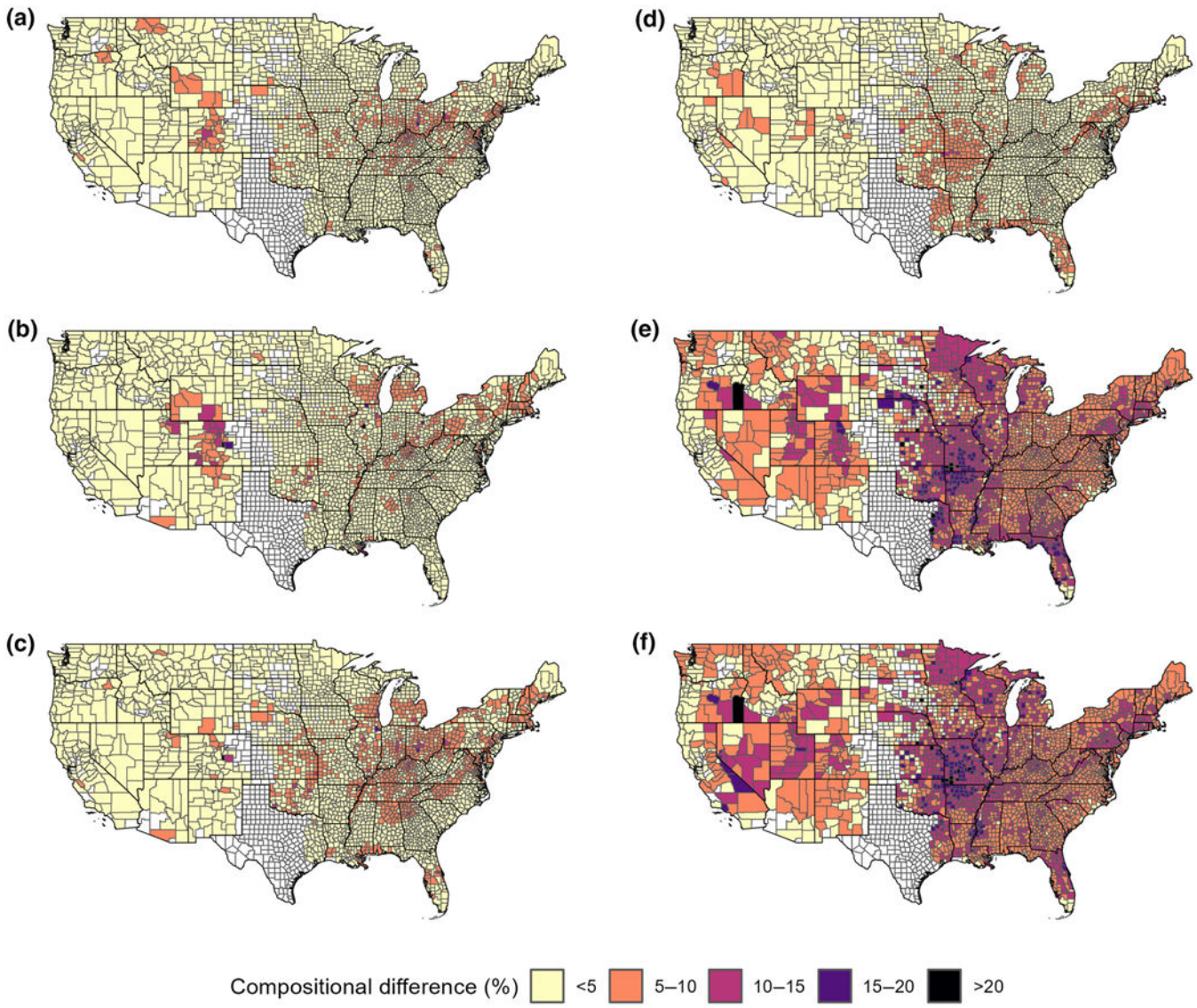

Fig. 5. Spatial patterns in compositional differences among scenarios.

Shown are the differences in total composition (eqn. 1) in 2100 at the county level for deposition scenarios under a constant climate with N reduction (a), S reduction (b) and N+S reduction (c) relative to no changes in deposition; and for climate scenarios with reduction in N and S deposition under scenarios $C_{4.5}$ (d), $C_{8.5,\ wet}$ (e), and $C_{8.5,\ dry}$ (f) relative to the constant climate scenario (counties in white do not have FIA plots that are forested). Map lines delineate study areas and do not necessarily depict accepted national boundaries.

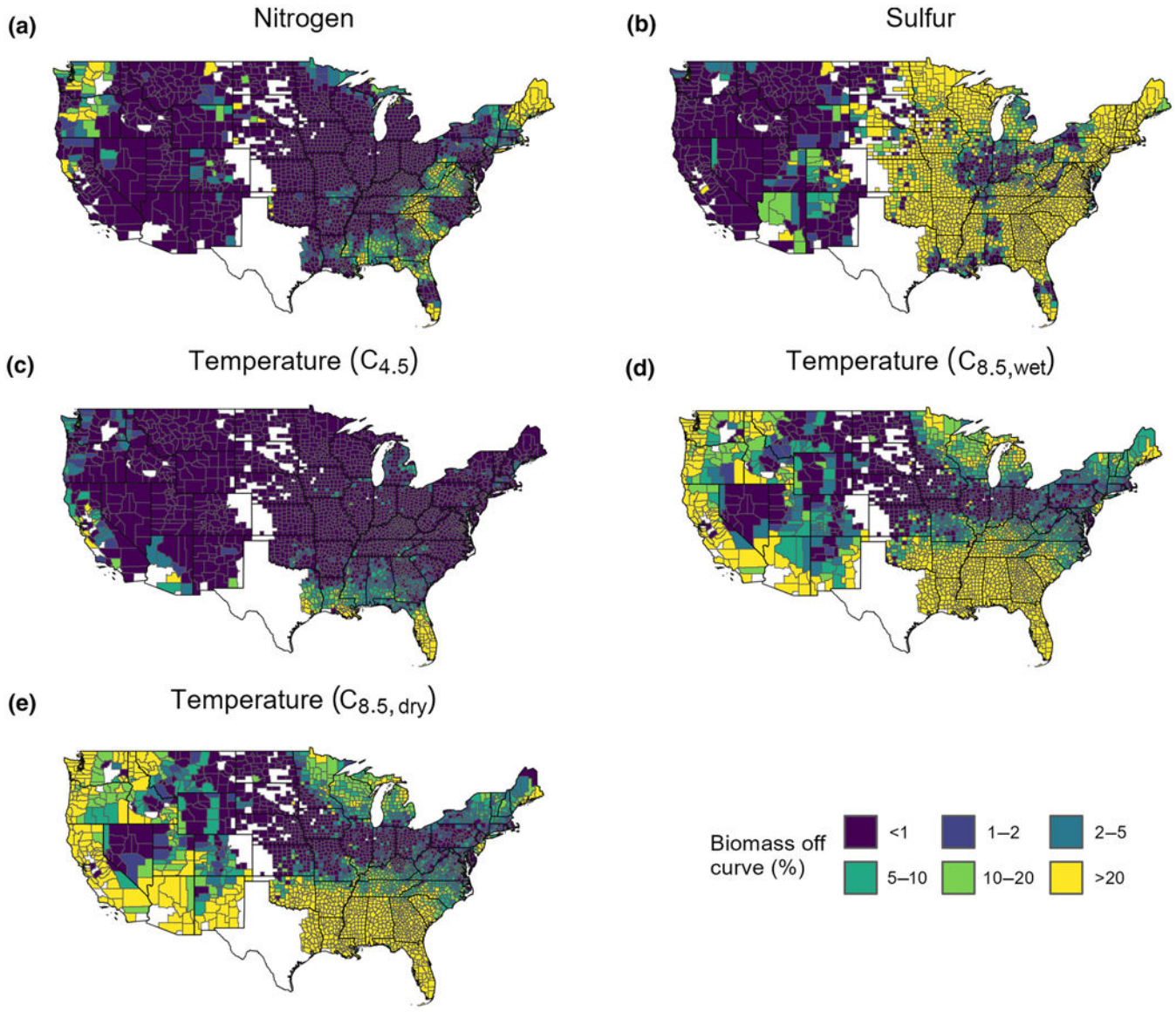

Fig. 6: Basal area off the curves.

Distribution of tree basal area by county that is projected to be outside of the 2000–2016 record by the year 2100 for minimum N deposition under the N reduction scenario (a), minimum S deposition under the S reduction scenario (b), and maximum temperature for scenarios $C_{4.5}$ (d), $C_{8.5,\ wet}$ (e) and $C_{8.5,\ dry}$ (f), respectively. Map lines delineate study areas and do not necessarily depict accepted national boundaries.